

Geochemistry Characteristics of Source Rocks and Oil–Source Correlation in the Gaosheng Area of the Western Depression in the Liaohe Basin, Northeastern China

Guangjie Zhao, Fujie Jiang,* Hong Pang, Xingzhou Liu, Chang Chen, and Di Chen



Cite This: *Energy Fuels* 2023, 37, 18855–18866



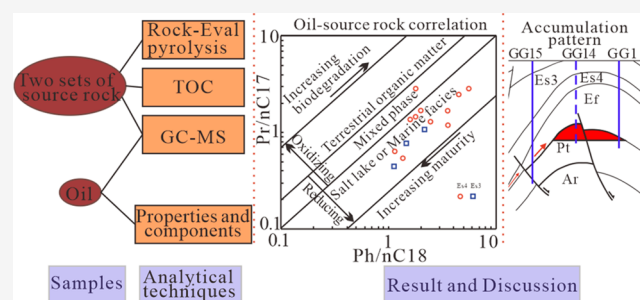
Read Online

ACCESS |

Metrics & More

Article Recommendations

ABSTRACT: The hydrocarbon generation potential of source rocks in the high-rise area of the Western Depression of the Liaohe Basin is high. However, the source of the oil is still unclear. The characteristics of source rocks and crude oil are analyzed by rock pyrolysis and saturated hydrocarbon chromatography–mass spectrometry, and then the oil–source correlation is determined. The results show that the crude oil in the Gaosheng area mainly comes from the Es4 (Shahejie Member 4) source rocks. A comparison of the oil and source rock correlation provides direct evidence to identify oil transport systems. The source material of Es4 source rocks is diverse and deposited in a weakly reductive to reductive brackish environment. It is formed by the double input of terrigenous higher plants and aquatic organisms, and the higher plants are the main source. The evaluation results show that Es4 contains mainly type II₁ and type II₂ kerogen, which are medium to good source rocks. The oil generation potential is 2.5×10^6 – 50×10^6 t/km², indicating that the source rocks have sufficient hydrocarbon supply capacity and have the potential to form large reservoirs. The results of this study have important reference significance for further study of the accumulation process of other blocks in the Liaohe Basin.



1. INTRODUCTION

With the transfer of oil and gas exploration from conventional to unconventional, tight sandstone oil and gas have become important areas of global gas production. Currently, the best tight oil exploration is in the United States, represented by the Bakken Formation in the Willingston Basin in North America.¹ The successful development of tight oil in America provides a good guide for the exploration of tight oil in the world. As a result, several tight oil reservoirs have been developed in Canada, Russia, India, Europe, and the Middle East.^{2–6} Tight oil reservoirs also exist in China, such as Ordos Basin,⁷ Tarim Basin,^{8,9} Sichuan Basin,¹⁰ Songliao Basin,¹¹ and Junggar Basin.^{12,13} However, the question of the source of the oil has not been well resolved. Because of the complex history of oil and gas injection, a single research method usually cannot provide reasonable results. Biomarker compounds and *n*-alkanes reflect the key characteristics of the original organic matter, so they are common in oil–source correlation research.^{14,15}

The Gaosheng oilfield is located in the north-central part of the Western Depression of the Liaohe Basin. Previous researchers have carried out much work on the Gaosheng oilfield, mainly focusing on the formation of the reservoir,¹⁶ the genetic mechanism of oil,¹⁷ oil reservoir features,¹⁸ controlling factors of accumulation,¹⁹ reservoir forming conditions,²⁰ and other aspects. Es3 and Es4 formations in the Gaosheng area are

considered potential source rocks.²⁰ However, due to the different degradation degrees of crude oil and the few exploration wells in the Gaosheng area, research on oil–source correlation is rare. Moreover, the thorough oil–source rock correlation poses obstacles to the analysis of hydrocarbon accumulation processes and severely limits the exploration and development of oil in the Gaosheng area.

The purpose of this study is to (1) characterize the hydrocarbon generation potential of Es3 and Es4 source rocks, (2) use biomarker compounds and *n*-alkanes to compare the characteristics of crude oil in the Gaosheng area with the source rocks to identify the oil source, and (3) point out the implications for oil accumulation. The research results will provide a reference for the exploration of surrounding oil reservoirs.

Received: August 18, 2023

Revised: November 2, 2023

Accepted: November 6, 2023

Published: November 20, 2023



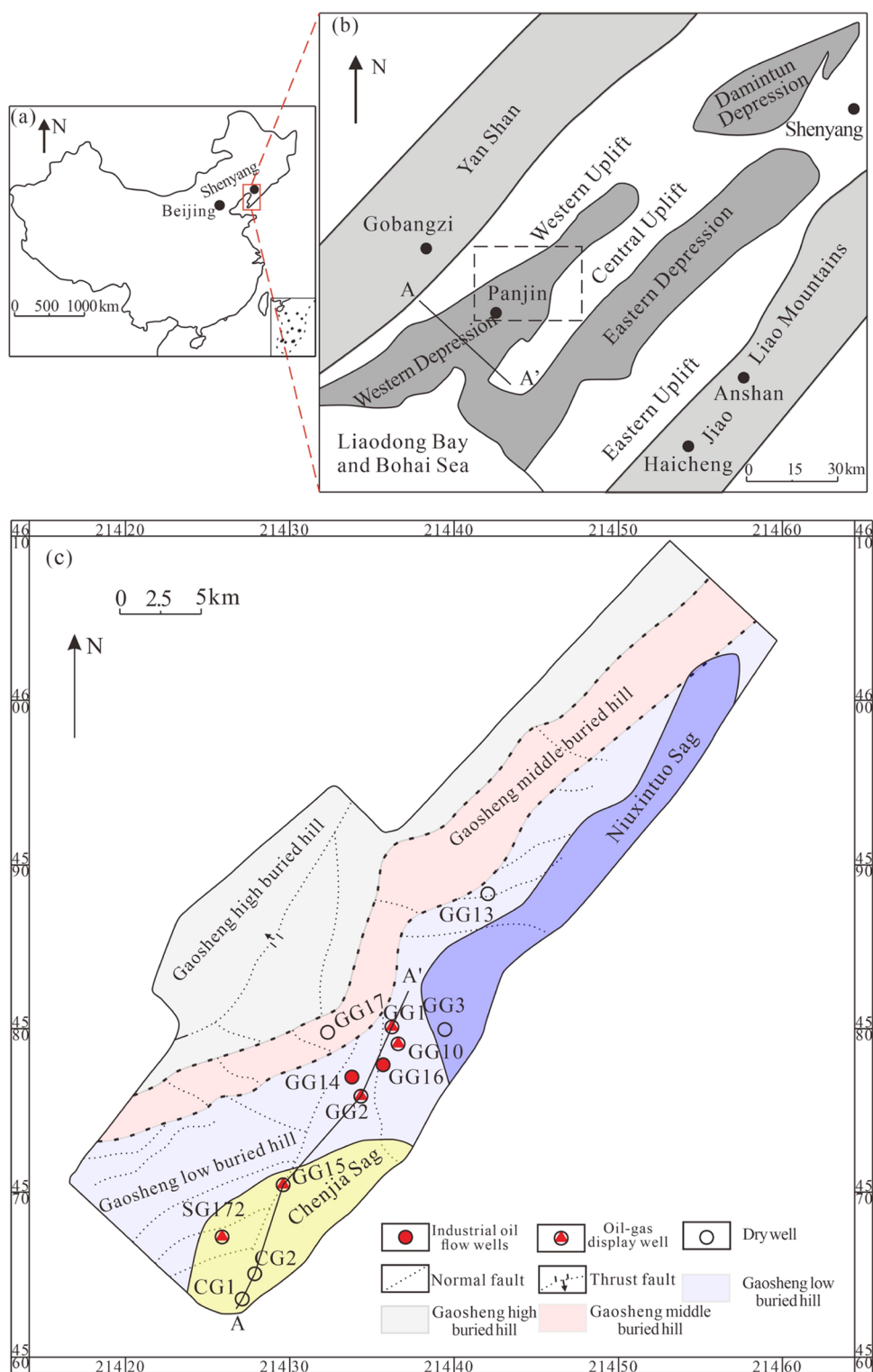


Figure 1. Comprehensive diagram of the stratigraphic and structural characteristics of the western Liaohe Basin.²⁵ (Reproduced with permission from ref 25. Copyright [2004] Wiley.) (a) Regional tectonic map of the Liaohe Basin, China. (b) Regional structure map of the Liaohe Basin indicating the geographical position of the Gaosheng area. (c) Structure map of the Gaosheng area and distribution of key exploration wells and oil fields.

2. GEOLOGICAL SETTING

Liaohe Basin, located in the northeast of Bohai Bay Basin, is a Mesocenozoic continental rift depression developed on the complex basement of the Pre-Mesozoic Era.²¹ It presents a “three depressions and three convex” tectonic pattern, namely, the Western Depression, Eastern Depression, Damintun

Depression, Western Uplift, Eastern Uplift, and Central Uplift (Figure 1).²² The Liaohe Basin is a Cenozoic fault depression of the North China platform. The regional tectonic evolution has undergone several stages, such as the formation of the Archean–Paleoproterozoic quasi-platform, the development of the Mesoproterozoic–Paleozoic quasi-platform cover, and the destruction and reconstruction of the Mesocenozoic quasi-

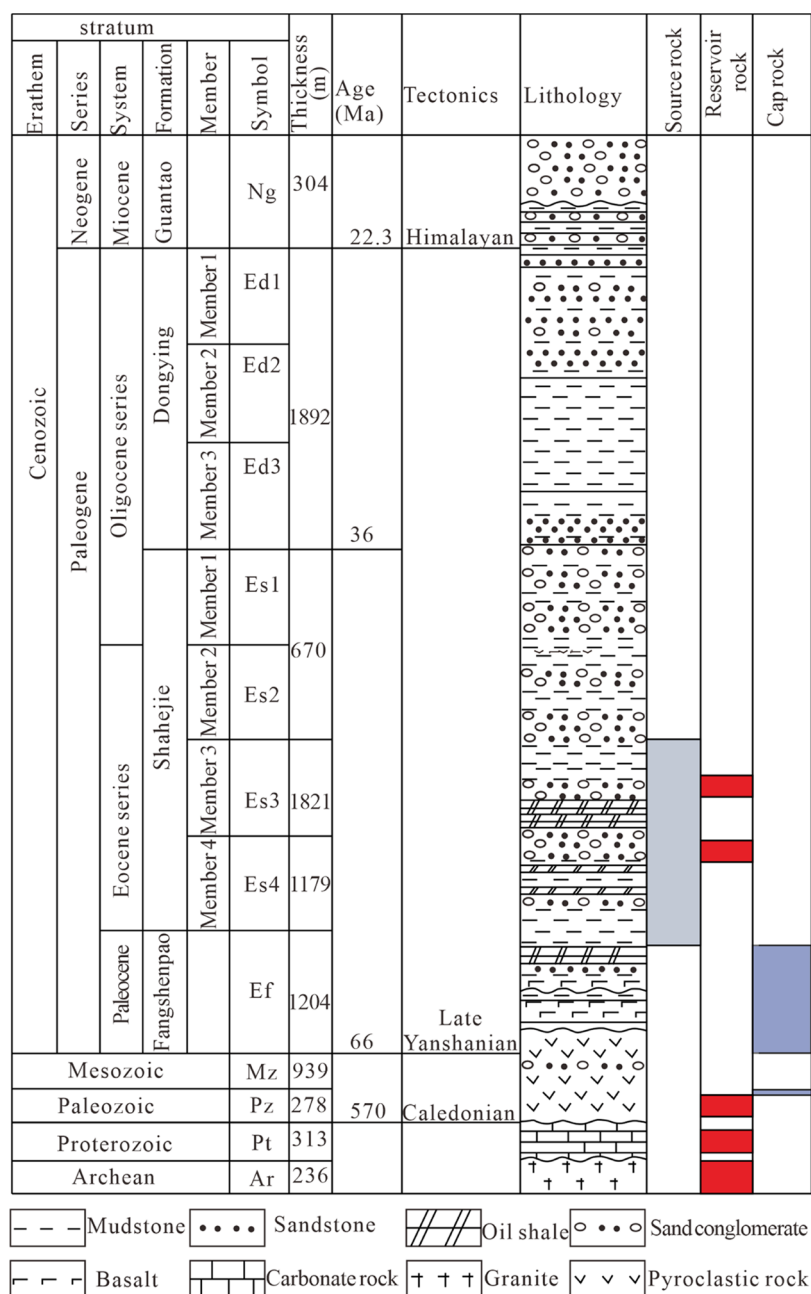


Figure 2. Comprehensive column chart of strata in the western Liaohe Basin.

platform. The Western Depression is a part of the Yanliaotai fold belt, and the formation of the present basement structure is a result of the superposition of multiple tectonic movements.²³ The basic tectonic pattern of the depression basement was formed by the strong east–west stretching movement in the Es3 (Shahejie Member 3) and Es4 (Shahejie Member 4) sedimentary stages of the Cenozoic Eocene. The western buried-hill belt was further uplifted by the right-lateral strike-slip caused by lateral compression stress in the late Oligocene, forming the present tectonic form.²⁴

The Gaosheng area is in the middle and north of the Western Depression. The strata developed from bottom to top include Archean, Proterozoic, Paleozoic, Mesozoic, and Cenozoic. Source rocks are developed in Es3 and Es4, reservoirs are mainly located in Proterozoic, and cap beds are mainly Mesozoic Fangshenpao Formation and Proterozoic volcanic rocks (Figure

2). The Gaosheng oilfield is located in the middle of the Gaosheng area. The fault and fracture development of the reservoir result from the orogenic movement, which can provide a good migration path for oil accumulation. Es3 and Es4 source rocks have great oil generation potential and can provide a lot of crude oil for reservoir generation.¹⁹

3. SAMPLES AND METHODS

The crude oil samples were separated and analyzed by gas chromatography–mass spectrometry (GC–MS). The shale samples were crushed and screened with an 80 mesh sieve. Total organic carbon (TOC) analysis was performed on the shale samples. Shale samples were extracted and fractionated by solvent organic matter, and saturated GC–MS was performed (Table 1).

The core samples were crushed to clean them. The TOC experiment was performed using a Leco CS-230 carbon analyzer. The pyrolytic analysis of rock was performed using an OGE-II rock pyrolyzer in the

Table 1. Data on Samples from the Gaosheng Area

well	layer	depth (m)	lithology	rock types
CG1	Es4	4024.2	mudstone	source rocks
CG2	Es3	3906.6		
CG1	Es3	3849.8		
CG2	Es4	3967.1		
GG2	Pt	2518.4	carbonate rock	oil
GG2	Pt	2697.8		
GG2	Pt	2741.9		
GG14	Pt	2160.2		
GG14	Pt	2190.3		
GG14	Pt	2420.5		
GG14	Pt	2642.6		
GG15	Pt	3695.3		
GG16	Pt	2675.6		
GG16	Pt	2679.6		

Key Laboratory of Petroleum and Gas, China University of Petroleum (Beijing). First, the instrument is heated until the temperature reaches the standard value, and then the experiment is started. When the temperature reaches 300 °C, the residual hydrocarbon is completely precipitated, and the fraction acquired at this temperature is S_1 . The hydrocarbon-generating material produced after cracking is S_2 . The highest pyrolysis temperature is T_{max} . The HI index was calculated according to the pyrolysis parameters. The ambient temperature is 10–30 °C. The ambient humidity is 1%–30%. High-purity helium pressures ranged from 0.20 to 0.30 MPa. The air pressure range is 0.30–0.40 MPa. The hydrogen pressure range is 0.20–0.30 MPa. The alternating current is 220 ± 10 v, 50 ± 3 Hz.

The physical properties of oil are provided by the Research Institute of Exploration and Development of the Liaohe Oilfield (RIEDLO).

The rock debris was treated into kerogen, and then the instantaneous cracking experiment was carried out. The saturated hydrocarbon GC–MS analytical instrument was a benchtop mass spectrometer Agilent 6890/5975, and the chromatographic column was an HP-5 ms quartz elastic capillary column (30 m × 0.25 mm × 0.25 μm). The heating procedure is set as follows: constant temperature at 50 °C for 1 min, followed by a temperature increase from 50 to 100 °C at 20 °C/min, and then from 100 to 315 °C at 3 °C/min. The temperature is then maintained at 315 °C for 16 min. The inlet temperature of helium was 300 °C with a flow rate of 1.00 mL/min. The detection method was full

scanning (50–550 amu) and multi-ion detection, and the ionization energy was 70 eV.

4. RESULTS

4.1. Characteristics of Source Rocks. **4.1.1. Distribution and Development Characteristics.** Two sets of Es4 and Es3 source rocks developed well in the Western Depression of Liaohe Basin.²⁶ Es4 source rocks are mainly oil shale and dark mudstone.²⁷ On the plane, the Es4 source rock in the Western Depression is thick in the north and thin in the south and the west. The thicknesses of the source rock in Niuxintuo Sag and Qingshui Sag are about 700 and 350 m, respectively. The thickness of the source rock in central Chenjia and Panshan Sag is 100–400 m (Figure 3a).²⁸ Es3 source rocks have a wide distribution area and large sedimentary thickness, which are thick in the south and thin in the north. Southern Qingshui Sag is the center of shale thickness, with a thickness of 700–1800 m (average 1200 m). In comparison, the average thickness of source rocks in Chenjia Sag and Niuxintuo Sag are up to 850 and 500 m, respectively (Figure 3b).²⁹

4.1.2. Geochemical Characteristics of Source Rocks. Evaluation indexes of organic matter abundance of source rocks generally include the TOC, potential hydrocarbon generation ($S_1 + S_2$), asphalt chloroform “A”, and total hydrocarbon (HC). This study mainly evaluates organic matter abundance based on TOC and the hydrocarbon generation potential. The average TOC of the Es3 source rock is only 0.19%, which is much lower than that of the Es4 source rocks (2.35%). According to the criteria,³⁰ the $S_1 + S_2$ value of mudstone is classified into non, poor, fair, good, and excellent grades. The $S_1 + S_2$ value of Es3 source rocks is 0.05–12.6 mg/g, which is mainly a fair source rock. The abundance of the Es4 source rock shows strong heterogeneity and is fair to good as a whole (Table 2 and Figure 4).

According to the rock pyrolysis data, type I and III kerogen can be seen in Es4 source rocks, but type II₁ and II₂ kerogen are dominant. The Es3 source rocks are mainly type II₁ and II₂, and type I is not developed (Figure 5).

R_o is a good index to characterize the maturity of source rocks.³¹ The R_o of the Es4 source rock ranges from 0.3% to

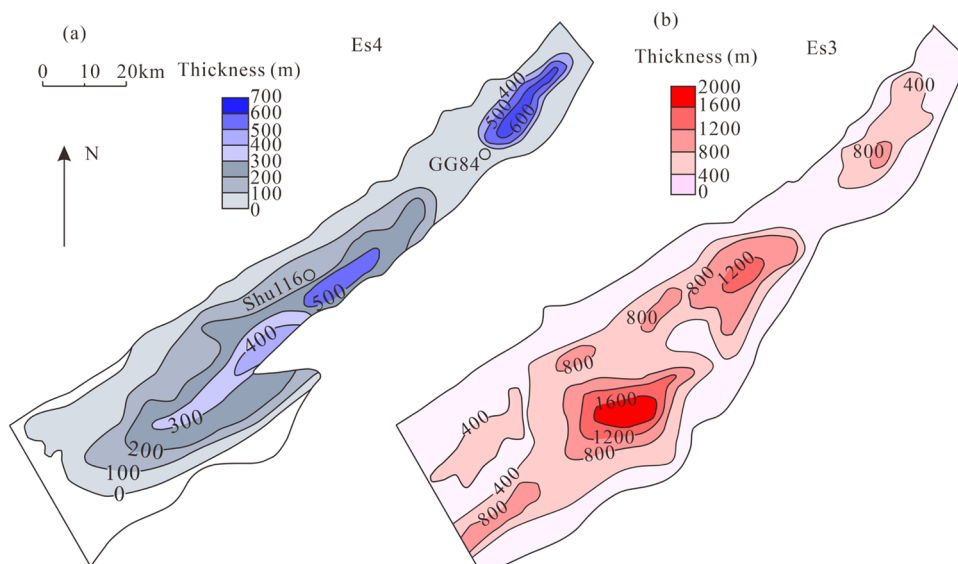


Figure 3. Thickness contour map of source rocks in the Western Depression: (a) Es4 Group and (b) Es3 Group.

Table 2. Data Table of Source Rock Geochemical Analysis of Shahejie Formation in the Western Depression of Liaohe Basin^a

layer	TOC (%)	S ₁ + S ₂ (mg/g)	HI (mg/g TOC)	T _{max} (°C)	vitrinite reflectance (R _o) (%)
Es3	0.03–1.19/0.19 (26)	0.05–12.6/1.6 (28)	73–92/84 (12)	432–445	0.28–1.29/0.68(39)
Es4	0.14–8.02/2.35 (26)	0.03–62.34/12.58 (24)	16–803/348 (58)	423–463	0.3–1.26/0.76 (37)

^aNote. Data: minimum–maximum/average value (number of samples).

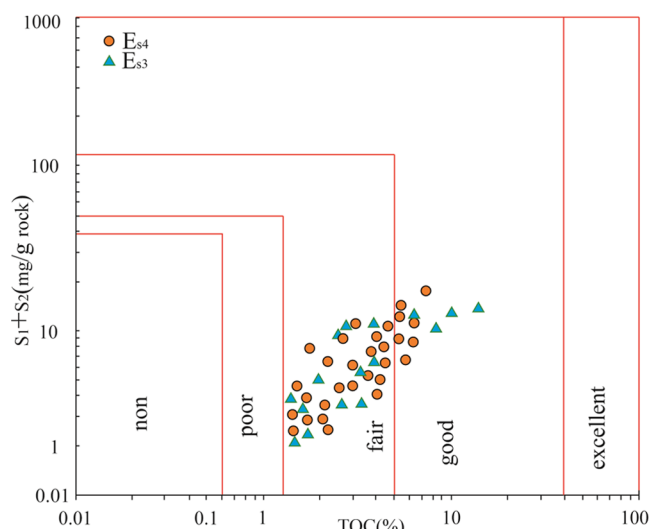


Figure 4. Organic matter abundance evaluation of Shahejie Formation source rocks in the Western Depression of the Liaohe Basin.

1.26% (average 0.76%). In comparison, the R_o of Es3 ranges from 0.28% to 1.29% (average 0.68%) (Figure 6). On the whole, the R_o value of the source rock increases obviously with an increase in the burial depth.

4.2. Physical Properties and Group Components of Crude Oil. Fluid physical properties can reflect the direction of the crude oil migration. To better understand the properties of crude oil, the oil test data of 4 industrial oil flow wells in the Gaosheng area are collated and analyzed. At 20 °C, the crude oil density is basically between 0.84 and 0.96 g/cm³. As can be seen in Table 3, the Gaosheng area is dominated by light oil.³² The viscosity ranges from 85.9 to 1446.3 mPa·s.

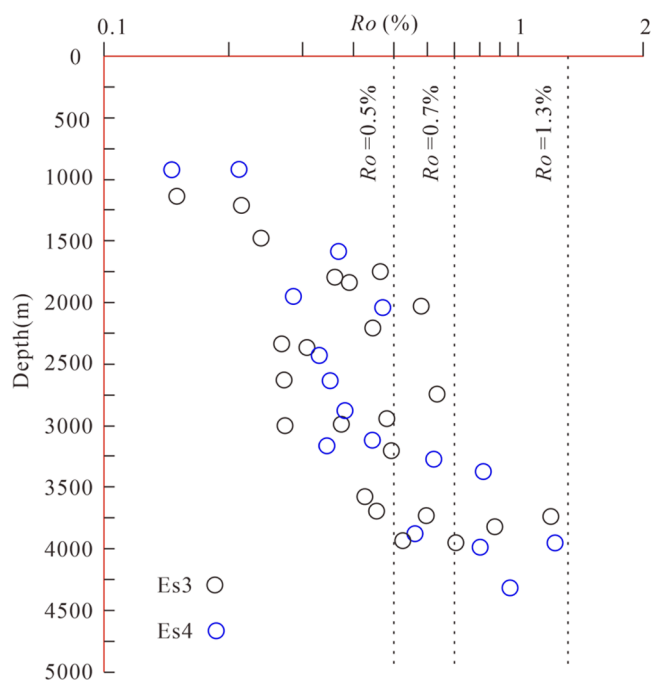


Figure 6. R_o values of Es3 + Es4 source rocks vary with depth in Chenjia Sag, the Western Depression of the Liaohe Basin.

The fraction composition data of crude oil samples are presented in Table 3. The samples were all normal fractions. The percentages of saturated hydrocarbon, aromatic hydrocarbon, asphaltene, and nonhydrocarbon were 61.6%–73.3%, 8.9%–15.8%, 6.5%–13.4%, and 5.6%–14.3%, respectively. Their average contents were 66.5%, 12.2%, 11.1%, and 10.2%, respectively (Table 3).

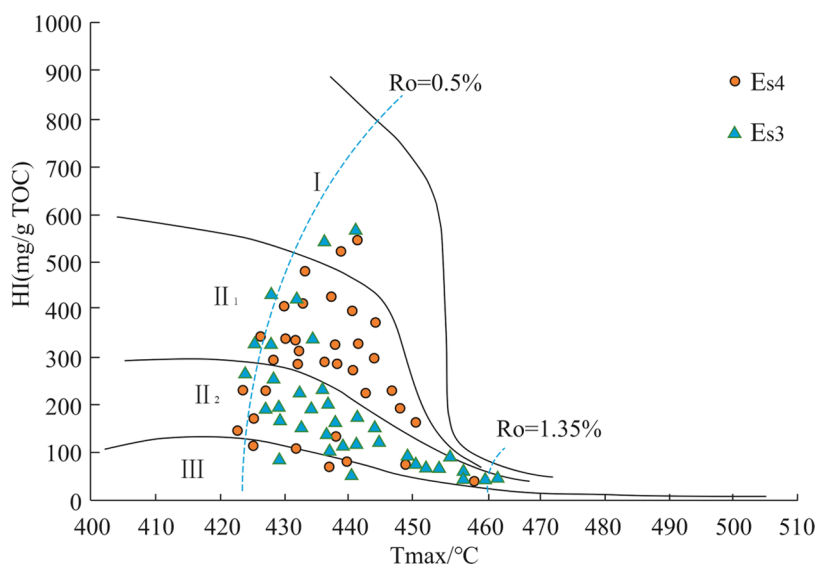


Figure 5. Classification chart of organic matter types of Shahejie source rocks in the Western Depression of the Liaohe Basin.

Table 3. Physical Properties of the Crude Oil in the Gaosheng Area

well	oil-bearing series	depth (m)	density/ $\text{g}\cdot\text{cm}^{-3}$ ($^{\circ}\text{C}$ @20 $^{\circ}\text{C}$)	viscosity/ $\text{mPa}\cdot\text{s}$ ($^{\circ}\text{C}$ @50 $^{\circ}\text{C}$)	saturated hydrocarbon	aromatic hydrocarbon	asphaltene	nonhydr-ocarbon
GG2	Pt	2518	0.87	85.9	64.5%	9.1%	12.1%	14.3%
GG2	Pt	2697	0.89	144.9	65.2%	10.9%	10.2%	13.7%
GG2	Pt	2741	0.89	1446.3	61.6%	12.8%	13.2%	12.4%
GG14	Pt	2160	0.84	88.27	64.5%	13.6%	12.6%	9.3%
GG14	Pt	2190	0.87	156.9	65.4%	15.6%	10.6%	8.4%
GG14	Pt	2420	0.87	1359.6	67.3%	15.8%	11.3%	5.6%
GG14	Pt	2642	0.96	86.7	69.7%	11.3%	12.5%	6.5%
GG15	Pt	3695	0.88	49.67	65.6%	9.8%	13.4%	11.2%
GG16	Pt	2675	0.8905	354	68.7%	12.5%	12.4%	6.4%
GG16	Pt	2679	0.8905	354	66.1%	13.6%	7.7%	12.6%
average value					66.5%	12.2%	11.1%	10.2%

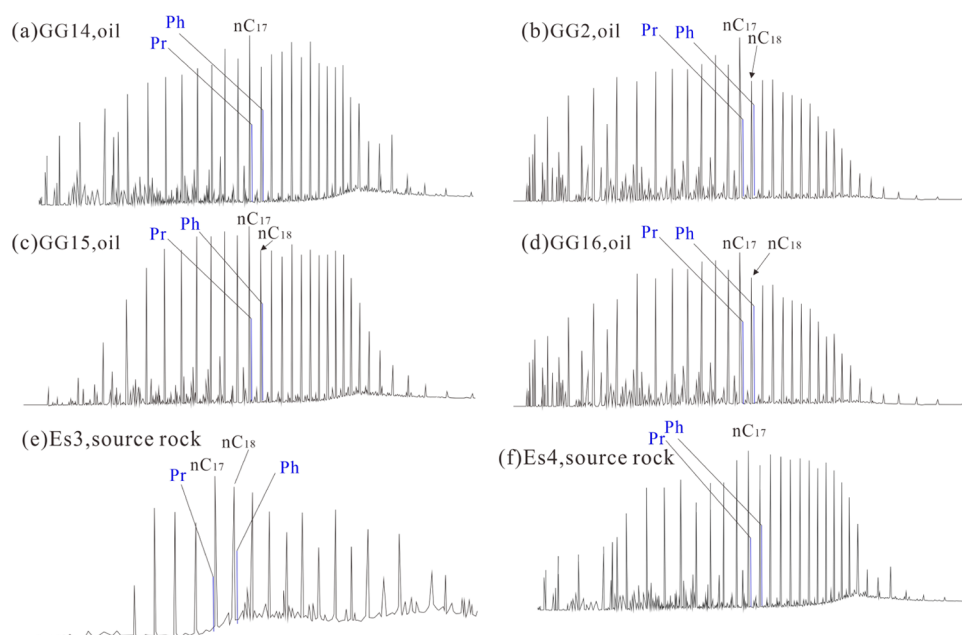
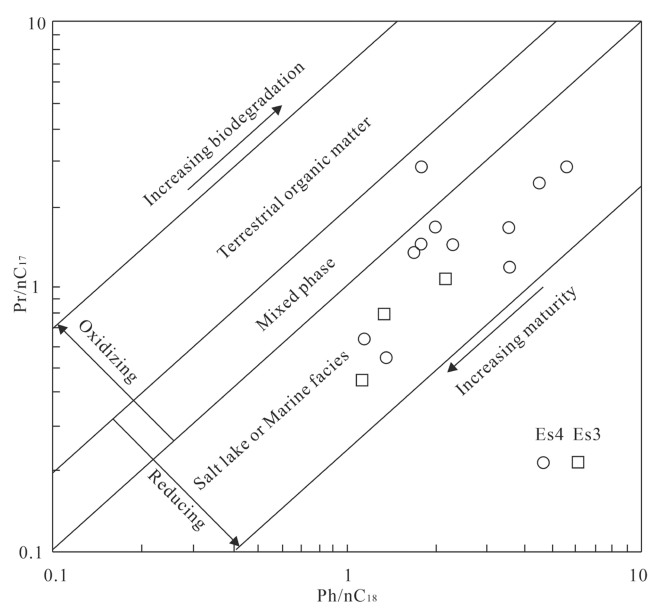


Figure 7. Chromatography–mass spectrum characteristics of crude oil and the source rock in the Gaosheng area.

4.3. Saturated Hydrocarbon Characteristics. The source of organic matter can be determined by the characteristics of *n*-alkanes.³² The ratios of Pr/Ph, Pr/ $n\text{C}_{17}$, and Ph/ $n\text{C}_{18}$ can reflect the sedimentary environment and maturity.³³ If the value of Pr/Ph is less than 0.5, it reflects a strong reducing paste salt environment; if the value of Pr/Ph is from 0.5 to 1, it reflects a reducing environment, and if the value of Pr/Ph is greater than 1, it indicates an oxidizing environment. The lower the values of Pr/ $n\text{C}_{17}$ and Ph/ $n\text{C}_{18}$, the higher the degree of thermal evolution of organic matter.^{34,35}

The main peak carbon of *n*-alkanes of oil in the Gaosheng area is C_{17} (Figure 7). The crude oil maturity is low, and its oil-generating parent material is deposited in a reducing brackish water environment (Figure 8). The *n*-alkanes of the Es4 source rocks in Chenjia Sag are bimodal, and the main peaks are C_{17} and C_{23} . Pr/ $n\text{C}_{17}$ ranged from 0.52 to 2.79, while Ph/ $n\text{C}_{18}$ ranged from 1.2 to 4.39, and the average Pr/Ph value was 0.84, indicating that the whole sample was in a weakly reductive to reductive brackish environment (Figure 8). The abundance of *n*-alkanes in Es3 source rock samples is low, and the main peak carbon is C_{17} . The Pr/Ph value was low (0.31). During the deposition of Es3, the depression was in the stage of drastic subsidence, forming a wide-deep-lake to a semi-deep-lake

Figure 8. Correlation diagram of Pr/ $n\text{C}_{17}$ and Ph/ $n\text{C}_{18}$ of Es3 and Es4 source rocks in the Western Depression.

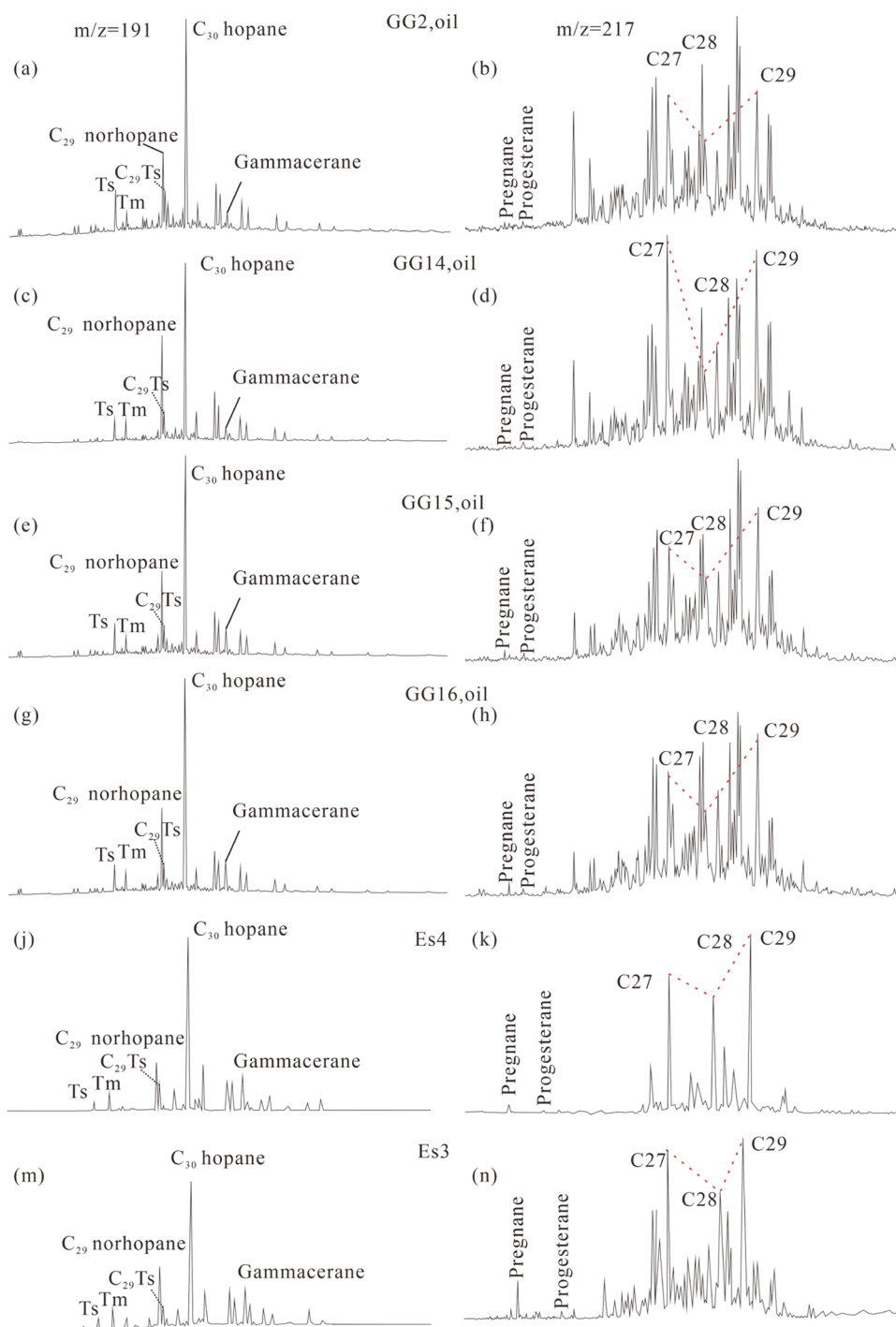


Figure 9. GC–MS analysis of the crude oil in the Gaosheng area. Oil samples from (a, b) well GG2, (c, d) well GG14, (e, f) well GG15, and (g, h) well GG16; mudstone samples from (j, m) GG1 and (k, n) GG2.

environment, and thick mudstone was deposited. Combined with Figure 8, this reflects that the Es3 source rock was formed in a reducing deep-water environment.^{36,37}

4.4. Characteristics of Sterane and Hopane. C_{27} – C_{28} – C_{29} regular steranes are commonly used to identify the source of parent materials. C_{27} steranes are mainly from lower aquatic organisms and algae, but C_{29} steranes are from terrestrial higher plants or diatoms and brown algae.³⁸ The maturity of organic matter can be reflected by aaa - $C_{29}20S/(20S + 20R)$, $C_{29}\beta\beta/(\beta\beta + aa)$, C_{31} hopane $22S/(22S + 22R)$, and Ts/Tm , and the ratio increases with an increase in maturity.³⁹ For domestic

continental sediments, the organic evolution stages of $\alpha\alpha$ - $C_{29}20S/(20S + 20R)$ parameters are less than 0.2 (immature), 0.2–0.3 (low maturity), and greater than 0.3 (mature).⁴⁰ Gammacerane is widely considered to be a marker of brackish depositional environments, and an increase in water salinity results in a high gammacerane index (gammacerane/ C_{30} hopane) and low Pr/Ph.³⁸

The steranes of Gaosheng crude oil mainly consist of C_{27} – C_{29} regular steranes, and the regular sterane distribution pattern includes “ $\sqrt{\quad}$ ” type ($C_{29} > C_{27} > C_{28}$) and “L” type ($C_{27} > C_{29} > C_{28}$). The crude oil in Pt formation is mainly “ $\sqrt{\quad}$ ” type,

accompanied by a small quantity of “L” type, and C₂₉ regular steranes dominate, which reflects that the oil source material is mainly higher plants, accompanied by a few lower aquatic organisms (Figure 9).

The ratio of regular steranes to 17 α (H)-hopanes indicates the contribution of eukaryotes (mainly algae and higher plants) and prokaryotes (bacteria) to the deposition of organic matter. Generally speaking, high regular sterane/hopane values (greater than 1) reflect marine organic matter of planktonic or benthic algae, while low regular sterane/hopane values (less than 1) reflect terrigenous or microbial modification.⁴⁰ The crude oil in the Gaosheng oilfield has low $\alpha\alpha\alpha$ -C₂₉20s/(20S + 20R), low C₂₉ $\beta\beta$ /($\beta\beta$ + $\alpha\alpha$), low Ts/Tm, and low (pregnane + pregnane)/ $\alpha\alpha\alpha$ -C₂₉20R, which reflect the low maturity of crude oil (Table 4). The high gammacerane index and regular sterane/hopane ratio of crude oil in the Gaosheng oil area indicate that the deposit is mainly a brackish water environment, and the oil-generating parent material may be mixed with algae (Figure 9a–h).

The distribution of C₂₇–C₂₈–C₂₉ regular steranes in Es4 source rocks is “√”, showing that the source material of oil generation is diverse, which is the dual input of higher plants and aquatic organisms. The peak value of C₃₀ hopane was the highest. The average values of $\alpha\alpha\alpha$ -C₂₉20s/(20S + 20R), C₂₉ $\beta\beta$ /($\beta\beta$ + $\alpha\alpha$), and C₃₁ hopane 22S/(22S + 22R) are 0.23, 0.26, and 0.53, respectively, and the value of Ts/Tm is 0.3, reflecting that the R_o of source rocks is low. The gammacerane index is 0.22, showing that Es4 source rocks were formed in saline water (Figure 9j,k).

The regular steranes of the Es3 source rock are “√” type. The values of $\alpha\alpha\alpha$ -C₂₉ 20S/(20S + 20R), C₂₉ $\beta\beta$ /($\beta\beta$ + $\alpha\alpha$), and C₃₁ hopane 22S/(22S + 22R) were 0.21, 0.36, and 0.54, respectively. The value of Ts/Tm is 0.62, and the value of gammacerane/C₃₀ hopane is 0.33, indicating that the Es3 source rock is dominated by the low-maturity and mature stages. The sedimentary environment is more saline than Es4 (Figure 9m,n).

5. DISCUSSION

5.1. Hydrocarbon Generation Potential of the Source Rocks.

The S₁ + S₂ value of the source rocks was evaluated based on the TOC content and rock pyrolysis parameters. All four wells reached oil window maturity.⁴¹ High TOC content and HI values indicate that the S₁ + S₂ value in this area is good. Types II₁ and II₂ are the dominant kerogen types and are consistent with previously published data from this formation (Figure 5).⁴² Changes in the TOC content and HI value indicate the heterogeneity of source rocks (Figures 4 and 5). Overall, the formations studied varied significantly in thickness, TOC content, and HI values. However, both sets contain intervals with high oil generation potential.

The oil generation range of the Western Depression almost covers the whole area, and the hydrocarbon generation intensity is between 2.5 × 10⁶ and 50 × 10⁶ t/km². The high-value areas of Es4 and Es3 are mainly in Niuxintuo Sag in the Shuguang area. The oil generation intensity of many large oil fields is greater than 3 × 10⁶ t/km² (Figure 10).^{43,44} This indicates that the source rocks in the Gaosheng area have a sufficient oil source and have the potential to form large reservoirs.

5.2. Oil and Source Rock Correlation.

5.2.1. Comparison of *n*-Alkane Characteristics.

By comparing the relative abundance of *n*-alkanes in the chromatogram of saturated hydrocarbons of the source rock and crude oil, the oil–source relationship can be intuitively compared. Proterozoic crude oil

Table 4. Composition Characteristics of Terpenoid Biomarkers in Crude Oil from the Western Liaohé Basin

well/source rock	gammacerane/C ₃₀ hopane	$\alpha\alpha\alpha$ -C ₂₉ S/(S + R)	C ₂₉ $\beta\beta$ ($\alpha\alpha$ + $\beta\beta$)	Ts/Tm	C ₃₁ hopane S/(S + R)	$\alpha\alpha\alpha$ -20R C ₂₇ /C ₂₉	regular sterane/hopane	(pregnane + progesterane)/ $\alpha\alpha\alpha$ -C ₂₉ 20R
GG2	0.29	0.25	0.23	0.26	0.55	0.65	1.12	0.03
GG14	0.18	0.24	0.21	0.23	0.57	0.71	1.08	0.11
GG15	0.17	0.21	0.24	0.20	0.56	0.87	1.09	0.13
GG16	0.25	0.26	0.19	0.24	0.58	0.74	1.06	0.14
Es4	0.22	0.23	0.26	0.3	0.53	0.82	1.09	0.08
Es3	0.33	0.21	0.36	0.62	0.54	0.76	1.11	0.12

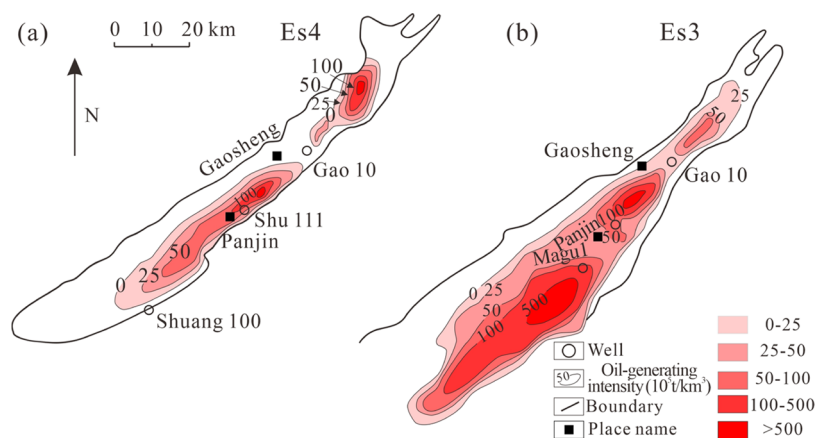


Figure 10. Hydrocarbon generation intensity diagram of Es3 and Es4 source rocks in the Western Depression of the Liaohe Basin (reproduced based on the data of the Liaohe Oilfield).

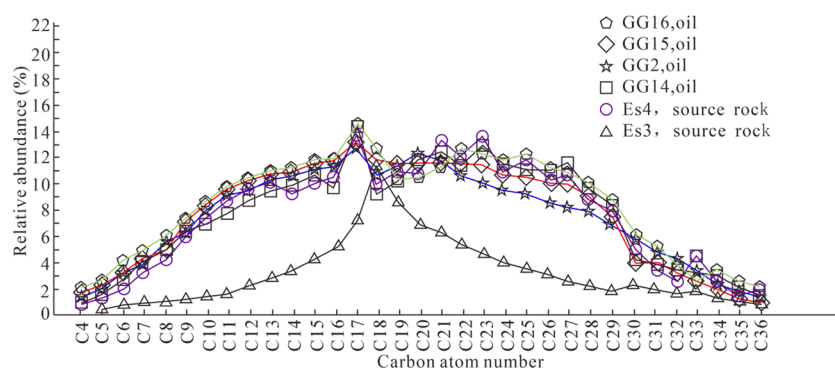


Figure 11. Comparison of distribution curves of oil–source *n*-alkanes in the Shahejie Formation of the Gaosheng area.

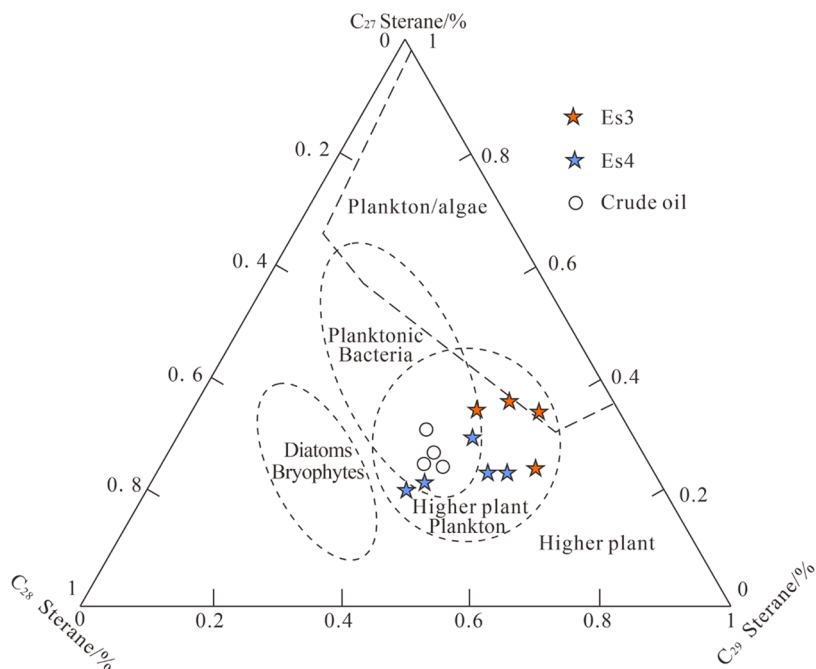


Figure 12. Comparison of oil–source Regular sterane content characteristics in the Shahejie Formation and Western Depression of Liaohe Basin.

in the Gaosheng area and Es4 source rock in Chenjia Sag show similar characteristics (Figure 11). The relative abundance of the main peak carbon nC_{17} was the highest, indicating a good relationship between the two.

5.2.2. Comparison of Biomarkers of Steranes. According to the analysis of the C_{27} – C_{29} – C_{28} regular sterane characteristics of Shahejie Formation crude oil in the Gaosheng area, combined with the proportion of composition of the crude oil family, it is

concluded that the hydrocarbon generation parent material type of oil in the Gaosheng oilfield is mainly from the double input of lower aquatic organisms and terrigenous higher plants, and the latter dominates. By comparing regular sterane characteristics of oil and source rocks of different strata, we recognize that the Proterozoic oil in the Gaosheng area has regular sterane characteristics similar to Es4 source rocks of Chenjia Sag, with a high gammacerane content and low Ts/Tm value, indicating that they have a good genetic relationship (Figures 9 and 12). Many previous scholars have used this method to compare oil sources.^{15,34,44}

5.3. Implication for Oil Accumulation. The Gaosheng reservoir is located in the hub of tectonic activity and has various trap types. It is a complex oil area with multiple layers, complex oil sources, and multiple oil charging. It is difficult to analyze the distribution and control factors of oil. Through a comparison of the oil source, various accumulation factors of the accumulation system can be studied. Combined with the characteristics of the regional geological evolution, the formation process of oil reservoirs can be finally revealed to clarify the exploration objectives. It has been proved that the accumulation characteristics of this accumulation system are relatively simple, which mainly shows the characteristics of single-source and two-stage charging.⁴⁵ The oil–source correlation plays a crucial role in simplifying complex issues.⁴⁶

The comparison of oil and source rock correlations provides direct evidence to identify oil transport systems. Through fine oil–source correlation, we can see that the characteristics of biomarkers of crude oil are consistent with those of Es4 source rocks. Because of the good regional cap rock conditions and numerous faults, oil migration is mainly lateral, with a long lateral migration distance and a large amount of oil migration (Figure 13). Through 3D seismic interpretation, it is confirmed

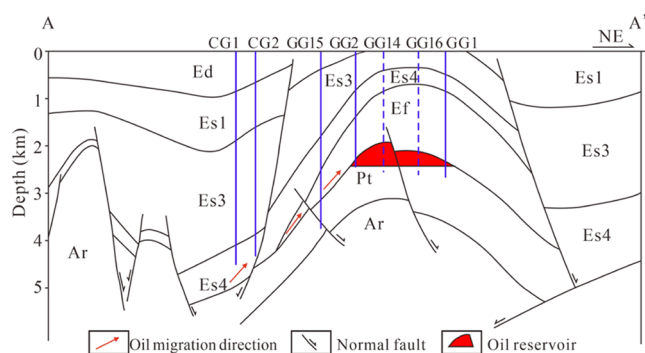


Figure 13. Reservoir accumulation pattern in the Gaosheng area (the profile is in Figure 1A–A').

that there are obvious faults in this area, which is conducive to connecting the Gaosheng reservoir and Es4 Source rock. Similar results have been found in previous studies.^{47,48}

6. CONCLUSIONS

The Gaosheng area is located in the middle north of the western depression, but its crude oil characteristics and oil sources are not clear. Therefore, *n*-alkane and sterane biomarker fingerprints were adopted to analyze the oil–source correlation.

The hydrocarbon generation range of the Western Depression almost covers the whole area, and the oil generation intensity is 2.5×10^6 – 50×10^6 t/km², which indicates that the

source rocks in the Gaosheng area have a sufficient oil supply capacity and the potential to form a large reservoir.

Based on the comparison between the *n*-alkane and sterane biomarker fingerprints of the crude oil and the source rocks, it is concluded that the crude oil comes from terrestrial lacustrine source rocks, but there are some differences in biomarkers between them. The results of biomarker oil–source correlation showed that the crude oil mainly came from the Es4 source rocks. The oil–source correlation provides a basis for determining the transport path of crude oil and then provides support for the analysis of the accumulation process.

AUTHOR INFORMATION

Corresponding Author

Fujie Jiang – College of Geoscience and State Key Laboratory of Petroleum Resource and Prospecting, China University of Petroleum (Beijing), Beijing 102249, China; orcid.org/0000-0002-0089-2972; Email: jfjhtb@163.com

Authors

Guangjie Zhao – College of Geoscience and State Key Laboratory of Petroleum Resource and Prospecting, China University of Petroleum (Beijing), Beijing 102249, China
 Hong Pang – College of Geoscience and State Key Laboratory of Petroleum Resource and Prospecting, China University of Petroleum (Beijing), Beijing 102249, China
 Xingzhou Liu – Petrochina Liaohe Oilfield Exploration and Development Research Institute, Panjin 124000 Liaoning, China
 Chang Chen – Petrochina Liaohe Oilfield Exploration and Development Research Institute, Panjin 124000 Liaoning, China
 Di Chen – College of Geoscience and State Key Laboratory of Petroleum Resource and Prospecting, China University of Petroleum (Beijing), Beijing 102249, China

Complete contact information is available at: <https://pubs.acs.org/10.1021/acs.energyfuels.3c03119>

Notes

The authors declare no competing financial interest.

ACKNOWLEDGMENTS

The authors thank engineers Zhi Tian and Yanmin Guo for their guidance and help. They are also grateful to the staff of the Exploration and Development Research Institute of Liaohe Oilfield of PetroChina for their assistance in collecting samples and providing some data. This research was financially funded by the Science Foundation of China University of Petroleum, Beijing (2462022XKBH005), and the China Postdoctoral Science Foundation (2022M723487).

REFERENCES

- (1) Brodie, M. W.; Aplin, A. C.; Hart, B.; Orland, I. J.; Valley, J. W.; Boyce, A. J. Oxygen Isotope Microanalysis By Secondary Ion Mass Spectrometry Suggests Continuous 300-million-year History of Calcite Cementation and Dolomitization in the Devonian Bakken Formation. *J. Sediment. Res.* **2018**, *88* (1), 91–104, DOI: [10.2110/jsr.2018.1](https://doi.org/10.2110/jsr.2018.1).
- (2) Friesen, O. J.; Dashtgard, S. E.; Miller, J.; Schmitt, L.; Baldwin, C. Permeability heterogeneity in bioturbated sediments and implications for waterflooding of tight-oil reservoirs, Cardium Formation, Pembina Field, Alberta, Canada. *Mar. Pet. Geol.* **2017**, *82*, 371–387.
- (3) Wüstefeld, P.; Hilse, U.; Koehrer, B.; Adelmund, D.; Hilgers, C. Critical evaluation of an Upper Carboniferous tight gas sandstone

reservoir analog: Diagenesis and petrophysical aspects. *Mar. Pet. Geol.* **2017**, *86*, 689–710.

(4) Hafiz, M.; Hakhoo, N.; Bhat, G. M.; Kanungo, S.; Ahmed, W.; et al. Source potential and reservoir characterization of the Cambay Shale, Cambay Basin, India: Implications for tight gas and tight oil resource development. *AAPG Bull.* **2020**, *104* (8), 1707–1749.

(5) Shilov, E.; Dorhjie, D. B.; Mukhina, E.; Zvada, M.; Kasyanenko, A.; Cheremisin, A. Experimental and numerical studies of rich gas Huff-n-Puff injection in tight formation. *J. Pet. Sci. Eng.* **2022**, *208*, No. 109420.

(6) Wei, C.; Li, Z.; Yang, J.; Liu, S.; Gao, Y. A comprehensive performance evaluation methodology for miscible gas flooding: A case study in a giant carbonate reservoir in Middle East. *J. Pet. Sci. Eng.* **2022**, *215*, No. 110668.

(7) Li, P.; Zheng, M.; Bi, H.; Wu, S.; Wang, X. Pore throat structure and fractal characteristics of tight oil sandstone: A case study in the Ordos Basin, China. *J. Pet. Sci. Eng.* **2017**, *149*, 665–674.

(8) Yang, H.; Wu, G.; Scarselli, N.; Sun, C.; Qing, H.; Han, J.; Zhang, G. Characterization of reservoirs, fluids, and productions from the Ordovician carbonate condensate field in the Tarim Basin, northwest China. *AAPG Bull.* **2020**, *104* (7), 1567–1592.

(9) Wang, Y.; Chen, J.; Pang, X.; Wang, G.; Hu, T.; Zhang, B.; Huo, Z.; Chen, H. Hydrocarbon migration along fault intersection zone - A case study on Ordovician carbonate reservoirs in Tazhong area, Tarim Basin, NW China. *Geol. J.* **2017**, *52* (5), 832–850.

(10) Deng, J.; Liu, M.; Ji, Y.; Tang, D.; Zeng, Q.; Song, L.; Tan, X.; Zeng, W.; Lian, C. Controlling factors of tight sandstone gas accumulation and enrichment in the slope zone of foreland basins: The Upper Triassic Xujiahe Formation in Western Sichuan Foreland Basin, China. *J. Pet. Sci. Eng.* **2022**, *214*, No. 110474.

(11) Er, C.; Zhao, J.; Li, Y.; Si, S.; Bai, Y.; Wu, W.; Han, Q. Relationship between tight reservoir diagenesis and hydrocarbon accumulation: An example from the early Cretaceous Fuyu reservoir in the Daqing oil field, Songliao Basin, China. *J. Pet. Sci. Eng.* **2022**, *208*, No. 109422.

(12) Zhao, P.; Wang, Z.; Sun, Z.; Cai, J.; Wang, L. Investigation on the pore structure and multifractal characteristics of tight oil reservoirs using NMR measurements: Permian Lucaogou Formation in Jimusaer Sag, Junggar Basin. *Mar. Pet. Geol.* **2017**, *86*, 1067–1081.

(13) Hu, T.; Pang, X.; Wang, X.; Pang, H.; Liu, Y.; Wang, Y.; Tang, L.; Chen, L.; Pan, Z.; Xu, J.; Pang, Y. Tight oil play characterisation: the lower – middle Permian Lucaogou Formation in the Jimusaer Sag, Junggar Basin, Northwest China. *Aust. J. Earth Sci.* **2016**, *63* (3), 349–365, DOI: 10.1080/08120099.2016.1203817.

(14) Zheng, R.; Zhang, G.; Qu, Y.; Wang, S.; Jin, X.; Chen, X.; Zhang, Z. Oil-source correlation under the complex geological conditions: A case study of the Chaiwopu Sag, southern Junggar Basin, NW China. *J. Pet. Sci. Eng.* **2022**, *210*, No. 110056.

(15) Alizadeh, B.; Maroufi, K.; Fajrak, M. Oil-oil correlation, geochemical characteristics, and origin of hydrocarbons from Mansourabad oilfield, SW Iran. *J. Afr. Earth Sci.* **2018**, *147*, 383–392, DOI: 10.1016/j.jafrearsci.2018.06.008.

(16) Dong, C.; Lin, C.; Hou, L.; Xin, Q.; Liu, Z. Genesis, distribution and formation conditions of sandstone rock mass in reservoir—A case study of the second and third block of Gaosheng Oilfield in Western Liaohe Sag. *Pet. Geol. Exp.* **1996**, Vol. 18 3, pp 289–297.

(17) Li, S.; Pang, X.; Gao, X.; Liu, K.; Li, X.; Chen, Z.; Liu, B. Genetic mechanism of heavy oil in western Liaohe Depression. *Sci. China Earth Sci.* **2008**, *51*, pp 138–149.

(18) Li, X.; Jin, K.; Zhou, Y. Characteristics of lacustrine carbonate reservoir in the fourth member of Shahejie Formation in Lejia area. *Spec. Oil Gas Reserv.* **2016**, Vol. 23 4, pp 25–28.

(19) Yu, J. *Main Controlling Factors and Objective Evaluation of Hydrocarbon Accumulation in Gaosheng Proterozoic Buried Hill*; Northeast Petroleum University: Daqing, 2016.

(20) Wu, C. *Analysis of Hydrocarbon Accumulation Conditions and Evaluation of Favorable Targets in Gaosheng Buried Hill*; Northeast Petroleum University: Daqing, 2012.

(21) Li, W.; Zhang, J.; Jing, T.; Ge, M.; Sun, R. Shale oil accumulation conditions and optimal selection of favorable areas in western Liaohe Sag. *Spec. Oil Gas Reserv.* **2014**, Vol. 21 1, pp 59–63.

(22) Zhang, N.; Wu, Y.; Zhang, X.; Huang, S.; Li, T.; Zhang, X.; Lin, C.; Jiang, K.; Xia, C. Geochemical characteristics and geological significance of the third member of the Paleogene Shahejie Formation in Damin Tun sag, Liaohe Depression. *Acta Geol. Sin.* **2021**, Vol. 95 2, pp 517–535.

(23) Liu, J.; Liu, B.; Qian, B.; Zhang, H.; Chen, C. Basement structure and hydrocarbon accumulation characteristics of Western Depression. *Spec. Oil Gas Reserv.* **2009**, Vol. 16 1, pp 45–48.

(24) Ju, J. Characteristics of oil and gas transport system in buried-hill in Western Depression of Liaohe Depression. *Spec. Oil Gas Reserv.* **2022**, Vol. 29 4, pp 55–61.

(25) Fuhrmann, A.; Horsfield, B.; Lòpez, J. F.; Hu, L.; Zhang, Z. Organic facies, depositional environment and petroleum generating characteristics of the lacustrine Shahejie Formation, Es4 member, Western Depression, Liaohe Basin (NE China). *J. Pet. Geol.* **2004**, *27* (1), 27–46.

(26) Mao, J.; Jing, T.; Han, X.; Shang, C.; Huang, S.; Ma, M. Petrological types and organic geochemical characteristics of high quality shale segments in western Liaohe Depression. *Earth Sci. Front.* **2016**, Vol. 23 1, pp 185–194.

(27) Shan, Y. *Accumulation Conditions and Distribution of Paleogene Shale Oil and Gas in Liaohe Depression*; China University of Geosciences: Beijing, 2013.

(28) Hu, Y.; Wang, Y.; Huang, S.; Wang, Q.; Liu, H. Petroleum geological conditions, resource potential and exploration direction in Liaohe Depression. *Mar. Origin Pet. Geol.* **2019**, Vol. 24 2, pp 43–54.

(29) Wang, Y.; Hu, Y.; Huang, S.; Kang, W.; Chen, Y. Geological conditions, resource potential and exploration direction of natural gas in Liaohe Depression, Bohai Bay Basin. *Nat. Gas Geosci.* **2018**, Vol. 29 10, pp 1422–1432.

(30) Chen, J.; Zhao, C.; He, Z. Criteria for evaluating the hydrocarbon generating potential of organic matter in coal measures. *Pet. Explor. Dev.* **1997**, *24* (1), 1–5.

(31) Wang, Y.; Cao, J.; Tao, K.; Li, E.; Ma, C.; Shi, C. Reevaluating the source and accumulation of tight oil in the middle Permian Lucaogou Formation of the Junggar Basin, China. *Mar. Pet. Geol.* **2020**, *117*, No. 104384.

(32) Youshu, B.; Yongshi, W.; Zheng, L.; Shouchun, Z.; Rifang, Z.; Lianbo, W. Accumulation conditions for deep light oil and condensate gas from Member 4 of Shahejie Formation in Jiyang depression. *Acta Pet. Sin.* **2021**, *42* (12), 1615–1624, DOI: 10.7623/syxb202112007.

(33) Peters, K.; Moldowan, J. *The Biomarker Guide-Interpreting Molecular Fossils in Petroleum*; Prentice Hall: NJ, 1993.

(34) Körmös, S.; Sachsenhofer, R. F.; Bechtel, A.; Radovics, B. G.; Milota, K.; Schubert, F. Source rock potential, crude oil characteristics and oil-to-source rock correlation in a Central Paratethys sub-basin, the Hungarian Palaeogene Basin (Pannonian basin). *Mar. Pet. Geol.* **2021**, *127*, No. 104955.

(35) Zhao, J.; Meng, X.; Han, Z. Near-source accumulation: Geochemical evidence of crude oil from the 6th Member of Yanchang Formation in the eastern margin of lacustrine basin of Yanchang Formation, Ordos Basin. *Acta Pet. Sin.* **2020**, Vol. 41 12, pp 1513–1526.

(36) Hao, F.; Zhou, X.; Zhu, Y.; Zou, H.; Yang, Y. Charging of oil fields surrounding the Shaleitian uplift from multiple source rock intervals and generative kitchens, Bohai Bay basin, China. *Mar. Pet. Geol.* **2010**, *27* (9), 1910–1926.

(37) Liu, X.; Xie, Q.; Xu, X.; Li, J.; Wang, L.; Song, Y. Sequence stratigraphy and sedimentary facies of Paleogene Shahejie Formation in the Eastern Sag of Liaohe Basin. *J. Northeast Pet. Univ.* **2015**, Vol. 39 6, pp 1–11.

(38) Moldowan, J. M.; Seifert, W. K.; Gallegos, E. J. Relationship Between Petroleum Composition and Depositional Environment of Petroleum Source Rocks. *AAPG Bull.* **1985**, *69* (8), 1255–1268, DOI: 10.1306/AD462BC8-16F7-11D7-8645000102C1865D.

(39) Zhang, L.; Bai, G.; Zhao, X.; Zhou, L.; Zhou, S.; Jiang, W.; Wang, Z. Oil-source correlation in the slope of the Qikou Depression in the

Bohai Bay Basin with discriminant analysis. *Mar. Pet. Geol.* **2019**, *109*, 641–657.

(40) Hou, D.; Feng, Z. *Petroleum Geochemistry*; Petroleum Industry Press: Beijing, 2011.

(41) Ghanizadeh, A.; Amann-Hildenbrand, A.; Gasparik, M.; Gensterblum, Y.; Krooss, B. M.; Littke, R. Experimental study of fluid transport processes in the matrix system of the European organic-rich shales: II. Posidonia Shale (Lower Toarcian, northern Germany). *Int. J. Coal Geol.* **2014**, *123*, 20–33.

(42) You, G.; Pan, J.; Zhang, K.; Liu, B.; Xiao, K. Analysis on hydrocarbon accumulation conditions of Paleogene in the northern Gaosheng area of the western sag of Liaohe Depression. *Acta Geol. Sin.* **2006**; Vol. 27 3, pp 241–246.

(43) Zhang, X.; Pang, H.; Pang, X.; Chen, J.; Wu, S.; Ma, K.; Zhang, S. Hydrocarbon generation and expulsion characteristics and resource potential of Upper Permian Longtan Formation source rocks in Sichuan Basin. *Oil Gas Geol.* **2022**; Vol. 43 3, pp 621–632.

(44) Jiang, Y.; Su, S.; Zhao, K. The relationship between fault transport capacity of oil source and hydrocarbon enrichment in non-hydrocarbon producing strata: A case study in Chengdao area of Bohai Bay Basin. *Acta Pet. Sin.* **2022**; Vol. 43 8, pp 1122–1131.

(45) Xu, B.; Guo, H.; Lin, T.; Qi, J.; Yang, H. Hydrocarbon accumulation periods in the western sag of Liaohe Depression. *Pet. Geol. Recov. Effic.* **2010**; Vol. 17 1, pp 12–14.

(46) Zhu, C.; Gang, W.; Zhao, X.; Chen, G.; Pei, L.; Wang, Y.; Yang, S.; Pu, X. Reconstruction of oil charging history in the multi-source petroleum system of the Beidagang buried-hill structural belt in the Qikou Sag, Bohai Bay Basin, China: Based on the integrated analysis of oil-source rock correlations, fluid inclusions and geologic data. *J. Pet. Sci. Eng.* **2022**, *208*, No. 109197.

(47) Hackley, P. C.; Dennen, K. O.; Garza, D.; Lohr, C. D.; Valentine, B. J.; Hatcherian, J. J.; Enomoto, C. B.; Dulong, F. T. Oil-source rock correlation studies in the unconventional Upper Cretaceous Tuscaloosa marine shale (TMS) petroleum system, Mississippi and Louisiana, USA. *J. Pet. Sci. Eng.* **2020**, *190*, No. 107015.

(48) Botterell, P. J.; Houseknecht, D. W.; Lillis, P. G.; Barbanti, S. M.; Dahl, J. E.; Moldowan, J. M. Geochemical advances in Arctic Alaska oil typing – North Slope oil correlation and charge history. *Mar. Pet. Geol.* **2021**, *127*, No. 104878.